
Neural networks for Anatomical Therapeutic Chemical (ATC)

Loris Nanni¹, Alessandra Lumini² and Sheryl Braham³

¹University of Padova, Via Gradenigo 6, Padova, Italy

²DISI, University of Bologna, via dell'Università 50, Cesena, Italy,

³Missouri State University, USA

Abstract

Motivation: Automatic Anatomical Therapeutic Chemical (ATC) classification is a critical and highly competitive area of research in bioinformatics because of its potential for expediting drug development and research. Predicting an unknown compound's therapeutic and chemical characteristics according to how these characteristics affect multiple organs/systems makes automatic ATC classification a challenging multi-label problem.

Results: In this work, we propose combining multiple multi-label classifiers trained on distinct sets of features, including sets extracted from a Bidirectional Long Short-Term Memory Network (BiLSTM). Experiments demonstrate the power of this approach, which is shown to outperform the best methods reported in the literature, including the state-of-the-art developed by the fast.ai research group.

Availability: All source code developed for this study is available at <https://github.com/LorisNanni>.

Contact: loris.nanni@unipd.it

1 Introduction

The average cost for developing a new drug from start to market, which can take decades before final approval, is now estimated to be 2.8 billion US dollars (Wouters, McKee, & Luyten, 2020). Of all drugs currently under development, approximately 86% (Pitts, 2014) will fail to be better than placebo or will prove to cause more harm than good. (Wong, Siah, & Lo, 2019). To weed out new drugs with a low probability of being efficacious and safe has led researchers to search for automatic methods for classifying compounds according to the organs they are likely to affect based on these compounds' Anatomical Therapeutic Chemical (ATC) classes. An automatic classification system with good ATC prediction would not only accelerate but also significantly reduce drug development costs.

The ATC coding system (MacDonald & Potvin, 2004) classifies compounds into one or more classes at five levels in terms of the therapeutic, pharmacological, and chemical properties of the drugs and on the organs or systems the drugs affect. Relevant to the automatic ATC classification problem is the first ATC level, which determines the general anatomical groups, as coded with fourteen mnemonic letters, that a particular compound targets: code **A** for alimentary tract and metabolism, **B** for blood and blood-forming organs, **C** for the cardiovascular system, **D** for dermatologicals, **G** for the genitourinary system and sex hormones, **H** for systemic hormonal preparations, excluding sex hormones and insulins, **J** for anti-infectives for systemic use, **L** for antineoplastic and immunomodulating agents, **M** for the musculoskeletal system, **N** for the nervous system,

P for antiparasitic products, insecticides, and repellents, **R** for the respiratory system, **S** for sensory organs, and **V** for various. Levels 2 and 3 represent pharmacological subgroups and levels 4 and 5 chemical subgroups and substances. A compound is assigned one or more ATC codes contained within each of these five levels.

Despite the serviceability of the ATC classification system for assessing the clinical value of a compound, most pharmaceuticals have yet to be assigned ATC codes; accurate coding involves expensive, labor-intensive experimental procedures. Hence, the pressing need for machine learning (ML) to be applied to this problem (Dunkel, Günther, Ahmed, Wittig, & Preissner, 2008; Wu, Ai, Liu, & Fan, 2013).

Early ML systems tended to simplify the complexity of this problem by reducing the level 1 multi-class problem to a single class problem. Dunkel et al. (2008), for example, took advantage of a compound's structural fingerprint information to identify a class, while Wu et al. (Wu et al., 2013) developed an approach based on extracting relationships among level 1 classes.

Chen et al. (2012) built one of the first multi-label systems by examining a compound's chemical-chemical interactions. The authors also established the de facto benchmark dataset for ATC classification. More recently, Cheng et al. (Cheng, Zhao, Xiao, & Chou, 2017a, 2017b) designed two systems (iATC-mHyb (2017a) and iATCmISF (2017b)) that handle class overlapping by fusing different sets of 1D descriptors: structural similarity, chemical-chemical interaction, and fingerprint similarity. Nanni and Braham (2017) transformed these same 1D descriptors into several 2D matrices from which Histogram of Gradients (HoG) (Dalal & Triggs, 2005) texture descriptors were extracted and trained on ensembles of multi-label classifiers. Convolutional Neural Networks (CNNs) were

trained on 2D descriptors in (Schmidhuber, 2015) and in (Lumini & Nanni, 2018), but in Lumini and Nanni (2018), the CNNs, along with a Long Short-Term Memory Network (LSTM) (Hochreiter & Schmidhuber, 1997), were used as feature extractors for training two multi-label classifiers. This approach was further expanded in Nanni, Brahnam, and Lumini (2017) by constructing ensembles of CNNs (with adjusted batch sizes and learning rates) and by introducing techniques for processing CNNs with multi-label inputs.

In this work, an ensemble of different feature descriptors and classifiers is proposed that strongly outperforms the best methods published in the literature for ATC classification on the benchmark dataset in Chen et al. (2012). The system proposed here was experimentally developed by comparing and evaluating multilabel classifiers trained on different feature sets. Our best results were obtained by combining a Bidirectional Long Short-Term Memory Network (BiLSTM) with a multi-label classifier based on Multiple Linear Regression.

2 Methods

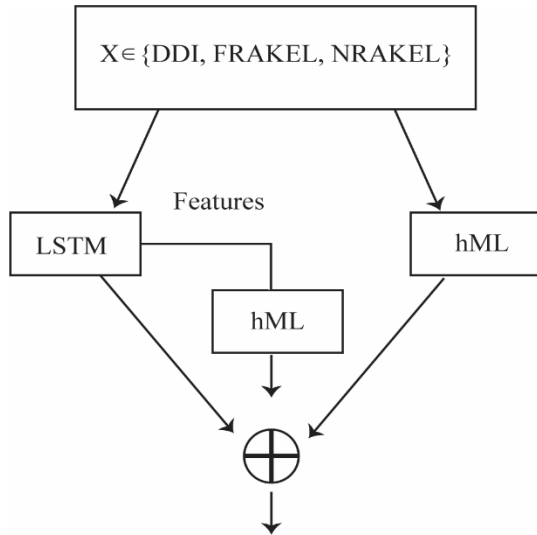


Fig. 1. Schematic of the proposed approach.

As illustrated in Figure 1, the approach taken in this study is to produce experimentally ensembles that combine multi-label classifiers (hML), based on Multiple Linear Regression, with LSTM. These classifiers are trained on X , a set of three different features (DDI, FRAKEL, NRAKEL, detailed in section 3.1). Sets of features are also extracted from LSTM and fed into hML classifiers. The results are combined and evaluated.

The remainder of this section describes each of the elements involved in this approach.

2.1 LSTM As Multi-label Classifier and Feature Extractor

LSTM (Hochreiter & Schmidhuber, 1997) is a Recurrent Neural Network that evaluates what to forget and what to remember at every step. As illustrated in Figure 2, is built with the following components: 1) forget gate f_t , which is a single layer network with sigmoid σ ; 2) candidate layer \bar{C}_t , which is a single layer network with $Tanh$; 3) input gate I_t , which is a

single layer network with σ ; 4) output gate O_t , which is a single layer network with σ ; 5) hidden state H vector; and 6) memory state C vector. The inputs to the LSTM at time step t are the current input X_t , the previous hidden state H_{t-1} , and the previous memory cell state C_{t-1} .

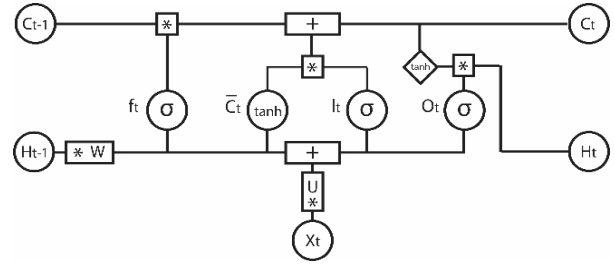


Fig. 2. Long Short-Term Memory (LSTM) classifier.

The algorithm for updating LSTM at time t is as follows:

Given X_t as the current input and H_{t-1} as the previously hidden layer and letting U, W, b , which represent the learnable weights of the network and are independent of time step t , the candidate layer \bar{C}_t is calculated as

$$\bar{C}_t = \text{Tanh}(U_c X_t + W_c H_{t-1} + b_c). \quad (1)$$

The new memory cell is a linear combination of the previous memory cell and of the candidate layer, such that

$$C_t = f_t * C_{t-1} + I_t * \bar{C}_t, \quad (2)$$

where $*$ is element-wise multiplication.

The forget gate f_t is defined as

$$f_t = \sigma(U_f X_t + W_f H_{t-1} + b_f); \quad (3)$$

the input gate I_t as

$$I_t = \sigma(U_i X_t + W_i H_{t-1} + b_i); \quad (4)$$

and the output gate as

$$O_t = \sigma(U_o X_t + W_o H_{t-1} + b_o). \quad (5)$$

The output of the block is the linear combination $H_t = O_t * \sigma(C_t)$ of the output gate O_t and the sigmoid of the memory cell C_t .

Regarding input, it should be noted that all sequences for this task are of the same length, so sorting input by length is not required. The output of LSTM can be the entire sequence H_t or the last term of this sequence. The former case makes it possible to stack many LSTM layers within the same network.

A Bidirectional LSTM (BiLSTM) is a stack of two LSTMs trained on the same data, with the second starting at the end of the first sequence and going backward. BiLSTM identifies causality correlations that go in the opposite direction and is usually applied to data that is not related to time.

MATLAB LSTM, which has one BiLSTM layer, was used to implement LSTM in this work. Parameters were set to the following values: $numHiddenUnits = 100$, $numClasses = 14$, and $miniBatchSize = 27$.

LSTM is not ordinarily used as a multilabel classifier but can perform multilabel classification if the training strategy in (Nanni et al., 2017) is implemented: if a training pattern belongs to m classes, it is replicated in the training set m times, once for each of the different labels. To assign a test pattern to more than one class, in the final softmax layer, a rule is applied that assigns a given pattern to all classes whose score is larger than a given threshold.

LSTM can function not only as a classifier but also as a feature extractor. As noted in Figure 1, in this study LSTM functions in both capacities. Feature extraction with LSTM can be accomplished by representing each pattern using the activations from the last layer, which produce a feature vector with a dimension equal to the number of classes. Feature perturbation and extraction are performed several times by randomly sorting the original set of features used to train LSTM.

2.2 Classification by hML

The novel algorithm hML-KNN, proposed in (P. Wang, Ge, Xiao, Zhou, & Zhou, 2017) is a multi-label classifier based on the integration of a feature score and a neighbor score. Feature score evaluates whether a sample belongs to a class based on its features according to the global information in the training data, while neighbor score determines this assignment based on the class labels of its neighbors. The feature score $f_1(x, g_j)$ for a given pattern x with respect to an anatomical group g_j is calculated to evaluate whether the pattern belongs to the group g_j based on a regression model. The neighbor score $f_2(x, g_j)$ is used to evaluate how significantly the K neighbors of a pattern belong to a given group g_j : the neighbor score increases if more neighbors of x have the label g_j . That is, $f_2(x, g_j)$ is 1 if all neighbors of x belong to g_j , 0 otherwise. The final score of x is a weighted sum of the two factors:

$$f(x, g_j) = \alpha f_1(x, g_j) + (1 - \alpha) f_2(x, g_j) \quad (6)$$

In our experiments, we use the default values where the weight factor α is set to 0.5, and the number of neighbors is $K=15$.

2.3 Classification by FastAI Tabular model

In addition to hML and LSTM, we explore the FastAI Tabular model (Howard & Gugger, 2020), which is a powerful deep learning technique for tabular/structured data based on the creation of some embedding layers for categorical variables. This deep learner uses embedding layers to represent categorical variables by a numerical vector, whose values are learned during training. Embeddings allow for relationships between categories to be captured, and they can also serve as inputs to other models.

A graphic representation of a FastAI Tabular model is presented in figure 3, where categorical variables are transformed into N -dimensional features by categorical embeddings followed by a dropout layer to prevent overfitting. Numerical variables are simply normalized. Then all the variables are concatenated and passed as input into the following layers, which, in our experiments, are two hidden and one output layers, as illustrated in Figure 3.

In our experiments, we used a binary encoding to represent binary variables, and we considered the resulting variable as categorical.

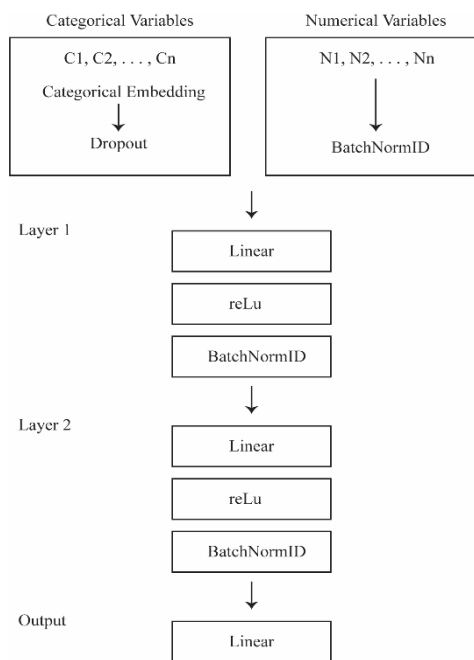


Fig. 3. FastAI Tabular model.

3 Results

3.1 Benchmark dataset

The ensembles generated by the proposed approach are compared and evaluated on the aforementioned benchmark dataset found in (Chen, 2012) (Supporting Information S1). This dataset is a collection of 3883 ATC-coded pharmaceuticals taken from KEGG (Ogata et al., 1999), a publicly available drug databank. Some samples belong to more than one of the 14 level 1 ATC classes: 3295 drugs belong to one class, 370 to two classes, 110 to three classes, 37 to four classes, 27 to five classes, and 44 belong to six classes.

As explained in (Chen, 2012), $N(\text{Vir})$ is the sum (4912) of labels associated with the drugs in the dataset. In other words, $N(\text{Vir})$ is the number of available virtual patterns, including all samples replicated in the training set with more than one label. The average number of labels per sample is thus $4912/3883=1.27$. A total of 540 samples belong to class **A**, 133 to **B**, 591 to **C**, 421 to **D**, 248 to **G**, 126 to **H**, 521 to **J**, 232 to **L**, 208 to **M**, 737 to **N**, 127 to **P**, 427 to **R**, 390 to **S**, and 211 to **V**.

The following descriptors represent each drug in this dataset:

- **DDI** represents each drug with three mathematical expressions (the maximum interaction score with the drugs, the maximum structural similarity score, and the molecular fingerprint similarity score) with each expression reflecting its intrinsic correlation with each of the 14 level 1 classes. Thus, the resulting descriptor is of size $14 \times 3=42$. These descriptors are available in the supplementary material in Nanni and Brahnam (2017).

- **FRAKEL** represents each drug by its ECFP fingerprint (Zhou, Chen, Wang, & Liu, 2020), which is a 1024-dimensional binary vector (available at <http://cie.shmtu.edu.cn/iatc/index>). The descriptor is obtained by feeding the drug (in the Simplified Molecular Input Line Entry System format) into RDKit (<http://www.rdkit.org/>), an open source chemistry informatics and machine learning toolkit. From this 1024-D binary vector, a 64-dimensional categorical descriptor is obtained, representing each group in 16 bits as an integer. This version of FRAKEL has been used with FastAI Tabular model.
- **NRAKEL** represents a drug by a 700-D descriptor obtained from the Mashup algorithm (Cho, Berger, & Peng, 2016) which generates output from seven drug networks (five based on chemical-chemical interaction and two on drug similarities).

3.2 Testing protocol

The jackknife testing protocol is used here to generate both the training and testing sets. At each iteration of this protocol, one sample is placed in the testing set and all the others are included in the training set. Iteration continues until every pattern has been left out from the training set exactly once. Results are averaged as in K-fold cross-validation. The jackknife protocol was selected because it is considered to be the least arbitrary cross-validation method commonly used in statistical prediction (Chou, 2013).

3.3 Performance indicators

ATC classification is evaluated using the classic performance indicators defined in (Chou, 2013):

$$\text{Aiming} = \frac{1}{N} \sum_{k=1}^N \left(\frac{\|\mathbb{L}_k \cap \mathbb{L}_k^*\|}{\|\mathbb{L}_k^*\|} \right), \quad (7)$$

$$\text{Coverage} = \frac{1}{N} \sum_{k=1}^N \left(\frac{\|\mathbb{L}_k \cap \mathbb{L}_k^*\|}{\|\mathbb{L}_k\|} \right), \quad (8)$$

$$\text{Accuracy} = \frac{1}{N} \sum_{k=1}^N \left(\frac{\|\mathbb{L}_k \cap \mathbb{L}_k^*\|}{\|\mathbb{L}_k \cup \mathbb{L}_k^*\|} \right), \quad (9)$$

$$\text{Absolute True} = \frac{1}{N} \sum_{k=1}^N \Delta(\mathbb{L}_k, \mathbb{L}_k^*), \quad (10)$$

$$\text{Absolute False} = \frac{1}{N} \sum_{k=1}^N \left(\frac{\|\mathbb{L}_k \cup \mathbb{L}_k^*\| - \|\mathbb{L}_k \cap \mathbb{L}_k^*\|}{M} \right), \quad (11)$$

where \mathbb{L}_k is the true label, with \mathbb{L}_k^* the predicted label for a given sample k . N is the number of samples, M the number of classes, and $\Delta(\cdot, \cdot)$ is an operator that returns 1 if the two sets have the same elements, 0 otherwise.

3.4 Experiments

The first experiment compares the performance of the multi-label classifiers. Reported in Table 1 are the results of the three multi-label classifiers detailed in section 3 along with three other standard classifiers, each trained on the three sets of features (DDI, FRAKEL, and NRAKEL). As already mentioned, LSTM is not a native multi-label classifier; thresholding was used as described in section 2.1 for this aim.

The six classifiers reported in Table 1 are the following:

- 1) RR, an ensemble of Ridge Regression classifiers implemented in the MATLAB/OCTAVE library for multi-class classification in the MLC Toolbox (Kimura, Sun, & Kudo, 2017);
- 2) LIFT, multi-label learning with Label specific Features (Zhang & Wu, 2015);

- 3) Group Preserving Label Embedding (GR) (Kumar, Pujari, Padmanabhan, & Kagita, 2019);
- 4) LSTM;
- 5) Tab (label for the FastAI Tabular model) (Howard & Gugger, 2020)
- 6) hML (P. Wang et al., 2017).

To avoid overfitting, default parameters were used for the classifiers.

Table 1. Absolute true rates achieved by different classifiers using different sets of descriptors

Absolute True	DDI	NRAKEL	FRAKEL
RR	0.5127	0.6062	0.5006
LIFT	0.6111	0.5282	0.3579
GR	0.4991	0.6093	0.4963
LSTM	0.6626	0.6585	0.6330
Tab	0.6441	0.7422	0.6760
hML	0.5710	0.6791	0.5977

In the cell Tab-FRAKEL, the reported value was obtained by transforming the original 1024 bit feature vector into 64 int16 features, since the original descriptor gained very low performance (0.3165)

Examining the results in Table 1, Tab is the best standalone approach producing an outstanding 0.7422 absolute true rate using NRAKEL descriptors. Of note as well is LSTM, which produced good on all three descriptors.

Table 2. Absolute true rates achieved by different ensembles using different set of descriptors

Absolute True	DDI	NRAKEL	FRAKEL
LS	0.6902	0.7092	0.6709
eLS	0.6995	0.7177	0.6853
LSTM+hML	0.6647	0.7371	0.6716
eLS+LSTM+hML	0.6915	0.7358	0.6894
eLS+LSTM+hML+Tab	0.6928	0.7538	0.7072

Table 3. Absolute true rates achieved by different ensembles using combinations of features.

Absolute True	DDI	NRAKEL	FRAKEL
Tab	0.7667	---	---
Tab	0.7734		
eLS+LSTM+hML	0.7577	---	---
eLS+LSTM+hML	0.7762		
eLS+LSTM+hML	0.7919		
+2×Tab			
eLS+LSTM+hML	0.8009		
+3×Tab			
LS+LSTM+Tab	0.7812		

The second experiment, reported in Table 2, considers the following ensembles:

- LS is a stacking method based on the approach described in section 2, where LSTM is used as a feature extractor and the resulting descriptors are given as input to a hML classifier;
- X+Y is fusion by the average rule between the methods X and Y;

Article short title

- eLS: is an ensemble based on feature perturbation obtained as the fusion of ten LS methods trained using random rearrangements of the input features;

Results reported in Table 2 show a strong performance improvement for descriptors trained on LS, which is a single hML classifier trained with LSTM features, to eLS, which is an ensemble of 10 LS classifiers. The best performance is obtained by the ensemble eLS+LSTM+hML+Tab, which is the fusion of methods that has the highest diversity compared to each other. This ensemble produces the highest performance in this classification problem, outperforming all the standalone approaches (for each of the three descriptors).

In the third experiment, fusion at the feature level is tested (see Table 3). The starting descriptor is the concatenation of two or three sets of features for the Tab approach, while for other classifiers, the combination is the average rule applied to each of them (e.g., LSTM, trained on DDI, is combined by average rule with LSTM, trained on NRAKEL).

When a cell in Table 3 spans more columns, that indicates that the related classifier is trained using more features, and, for each feature, a different classifier is trained with results combined by average rule.

The results reported in Table 3 show the usefulness of the ensemble: all the approaches that contain Tab outperform the state of the art produced by the fast.ai research group.

Table 4. Comparison with the state-of-the-art methods in the literature

Method	Aiming	Coverage	Accuracy	Absolute True	Absolute False
eLS+ LSTM+hML +3*Tab	0.9139	0.8432	0.8338	0.8009	0.0131
Chen et al. (2012)	0.5076	0.7579	0.4938	0.1383	0.0883
iATC-mHYb (Cheng et al., 2017a)	0.7191	0.7146	0.7132	0.6675	0.0243
iATC-mISF (Cheng et al., 2017b)	0.6783	0.6710	0.6641	0.6098	0.0585
EnsLIFT (Nanni & Brahnam, 2017)	0.7818	0.7577	0.7121	0.6330	0.0285
EnsANET_LR (Lumini & Nanni, 2018)	0.7536	0.8249	0.7512	0.6668	0.0262
iATC_Deep-mISF (Lu & Chou, 2020)	0.7470	0.7391	0.7157	0.6701	0.0000
NRAKEL (Zhou, Chen, & Guo, 2019)	0.7888	0.7936	0.7786	0.7593	0.0363
FRAKEL (Zhou et al., 2020)	0.7851	0.7840	0.7721	0.7511	0.0370
NLSP (X. Wang, Wang, Xu, Xiong, & Wei, 2019)	0.8135	0.7950	0.7828	0.7497	0.0343
FUS3 (Nanni et al., 2017)	0.8755	0.6973	0.7346	0.6871	0.0238

Finally, in Table 4, we report a comparison of our proposed method with the best systems reported in the literature. Clearly, our ensemble strongly outperforms the other approaches. Notice the performance difference of the original papers of NRAKEL (Zhou et al., 2019) and FRAKEL (Zhou et al., 2020) and the classifiers tested here. The main reason for this difference is that the classifiers were not optimized here since we are using a single dataset. Our concern in this regard is to avoid any risk of overfitting by running the approaches using default values.

Conclusion

Since automatic level 1 ATC classification is a complex multi-label problem, the goal of this study was to improve performance by generating ensembles trained on three different feature vectors. The original 1D input vectors were also used to train an LSTM (specifically a BiLSTM), which functioned (with modification) not only as a multi-label classifier but also as a feature extractor, with features taken from the output layer.

Two other classifiers aside from LSTM were evaluated: one based on Multiple Linear Regression and another a deep learning technique for tabular/structured data based on the creation of some embedding layers for categorical variables. To boost the performance of these classifiers they were trained on three sets of features with results combined by the average rule. Comparisons of the best ensembles were made with the standalone classifiers and other state-of-the-art systems. Experimental results show that the best ensemble constructed by the method proposed here obtained

superior results across the five performance indicators for ATC classification, including the systems introduced in Lumini and Nanni (2018), Nanni et al. (2017), and the fast.ai research group.

Future work will explore performance of different LSTM and CNN topologies combined with new activation functions for replacing the standard ReLu. The fusion of other deep learning topologies (using both the standard ReLu and variants) for extracting features will also be the focus of investigation.

The code of the proposed ensemble is available at <https://github.com/LorisNanni>.

Acknowledgement

Through their GPU Grant Program, NVIDIA donated the TitanX GPU that was used to train the CNNs presented in this work.

References

- Chen, L. (2012). Predicting anatomical therapeutic chemical (ATC) classification of drugs by integrating chemical-chemical interactions and similarities. *PLoS ONE*, 7(e35254).
- Cheng, X., Zhao, S.-G., Xiao, X., & Chou, K.-C. (2017a). iATC-mHyb: a hybrid multi-label classifier for predicting the classification of anatomical therapeutic chemicals. *Oncotarget*, 8, 58494–58503. doi:doi:10.18632/oncotarget.17028
- Cheng, X., Zhao, S.-G., Xiao, X., & Chou, K.-C. (2017b). iATC-mISF: a multi-label classifier for predicting the classes of anatomical

- therapeutic chemicals. *Bioinformatics*, 33(3), 341-346. doi:10.1093/bioinformatics/btw644
- Cho, H., Berger, B., & Peng, J. (2016). Compact Integration of Multi-Network Topology for Functional Analysis of Genes. *Cell Systems*, 3(6), 540-548.e545. doi:<https://doi.org/10.1016/j.cels.2016.10.017>
- Chou, K. C. (2013). Some remarks on predicting multi-label attributes in molecular biosystems. *Molecular Biosystems*, 9, 10922-11100.
- Dalal, N., & Triggs, B. (2005). *Histograms of oriented gradients for human detection*. Paper presented at the 9th European Conference on Computer Vision, San Diego, CA.
- Dunkel, M., Günther, S., Ahmed, J., Wittig, B., & Preissner, R. (2008). SuperPred: update on drug classification and target prediction. *Nucleic Acids Research*, 36(May), W55-W59.
- Hochreiter, S., & Schmidhuber, J. (1997). Long short-term memory. *Neural Computation*, 9(8), 1735-1780.
- Howard, J., & Gugger, S. (2020). Fastai: A Layered API for Deep Learning. *Information*, 11(2), 108. Retrieved from <https://www.mdpi.com/2078-2489/11/2/108>
- Kimura, K., Sun, L., & Kudo, M. (2017). MLC toolbox: A MATLAB/OCTAVE library for multi-label classification. *ArXiv*, arXiv:1704.02592.
- Kumar, V., Pujari, A. K., Padmanabhan, V., & Kagita, V. R. (2019). Group preserving label embedding for multi-label classification. *Pattern Recognition*, 90, 23-34. doi:<https://doi.org/10.1016/j.patcog.2019.01.009>
- Lu, Z., & Chou, K.-C. (2020). iATC_Deep-mISF: A Multi-Label Classifier for Predicting the Classes of Anatomical Therapeutic Chemicals by Deep Learning. *Advances in Bioscience and Biotechnology*, 11, 153-159.
- Lumini, A., & Nanni, L. (2018). Convolutional neural networks for ATC classification. *Current Pharmaceutical Design*, 24(34), 4007-4012. doi:<http://www.eurekaselect.com/167244/article>
- MacDonald, K., & Potvin, K. (2004). Interprovincial Variation in Access to Publicly Funded Pharmaceuticals: A Review Based on the WHO Anatomical Therapeutic Chemical Classification System. *Canadian Pharmacists Journal / Revue des Pharmaciens du Canada*, 137(7), 29-34. doi:10.1177/171516350413700703
- Nanni, L., & Brahnam, S. (2017). Multi-label classifier based on histogram of gradients for predicting the anatomical therapeutic chemical class/classes of a given compound. *Bioinformatics*, 33, 2837-2841. doi:10.1093/bioinformatics/btx278
- Nanni, L., Brahnam, S., & Lumini, A. (2017). *Ensemble of Deep Learning Approaches for ATC Classification*. Paper presented at the Smart Intelligent Computing and Applications - Proceedings of the Third International Conference on Smart Computing and Informatics, Bhubaneswar, India.
- Ogata, H., Goto, S., Sato, K., Fujibuchi, W., Bono, H., & Kanehisa, M. (1999). KEGG: Kyoto Encyclopedia of Genes and Genomes. *Nucleic Acids Research*, 27(1), 29-34. doi:10.1093/nar/27.1.29
- Pitts, R. C. (2014). Reconsidering the concept of behavioral mechanisms of drug action. *Journal of the Experimental Analysis of Behavior*, 101, 422-441. doi:doi:10.1002/jeab.80
- Schmidhuber, J. (2015). Deep learning in neural networks: An overview. *Neural Networks*, 61, 85-117.
- Wang, P., Ge, R., Xiao, X., Zhou, M., & Zhou, F. (2017). hMuLab: A Biomedical Hybrid Multi-LABEL Classifier Based on Multiple Linear Regression. *IEEE/ACM Trans. Comput. Biol. Bioinformatics*, 14(5), 1173-1180. doi:10.1109/tcbb.2016.2603507
- Wang, X., Wang, Y.-J., Xu, Z., Xiong, Y., & Wei, D.-Q. (2019). ATC-NLSP: Prediction of the Classes of Anatomical Therapeutic Chemicals Using a Network-Based Label Space Partition Method. *Frontiers in Pharmacology*, 10.
- Wong, C. H., Siah, K. W., & Lo, A. W. (2019). Estimation of clinical trial success rates and related parameters. *Biostatistics (Oxford, England)*, 20(2), 273-286. doi:10.1093/biostatistics/kxx069
- Wouters, O. J., McKee, M., & Luyten, J. (2020). Estimated Research and Development Investment Needed to Bring a New Medicine to Market, 2009-2018. *JAMA*, 323(9), 844-853. doi:10.1001/jama.2020.1166
- Wu, L., Ai, N., Liu, Y., & Fan, X. (2013). Relating anatomical therapeutic indications by the ensemble similarity of drug sets. *Journal of Chemical Information and Modeling*, 53(8), 2154-2160.
- Zhang, M.-L., & Wu, L. (2015). Lift: multi-label learning with label-specific features. *IEEE Transactions on Pattern Analysis and Machine Intelligence*, 37(1), 107-120.
- Zhou, J.-P., Chen, L., & Guo, Z.-H. (2019). iATC-NRAKEL: an efficient multi-label classifier for recognizing anatomical therapeutic chemical classes of drugs. *Bioinformatics*, 36(5), 1391-1396. doi:10.1093/bioinformatics/btz757
- Zhou, J.-P., Chen, L., Wang, T., & Liu, M. (2020). iATC-FRAKEL: a simple multi-label web server for recognizing anatomical therapeutic chemical classes of drugs with their fingerprints only. *Bioinformatics*, 36(11), 3568-3569. doi:10.1093/bioinformatics/btaa1166